Lyapunov exponent, mobility edges, and critical region in the generalized Aubry-André model with an unbounded quasiperiodic potential

Yi-Cai Zhang* and Yan-Yang Zhang
School of Physics and Materials Science, Guangzhou University, Guangzhou 510006, China

(Received 22 January 2022; revised 27 April 2022; accepted 28 April 2022; published 12 May 2022)

In this work, we investigate the Anderson localization problems of the generalized Aubry-André model (Ganeshan-Pixley-Das Sarma's model) with an unbounded quasiperiodic potential where the parameter $|\alpha| \geqslant 1$. The Lyapunov exponent $\gamma(E)$ and the mobility edges E_c are exactly obtained for the unbounded quasiperiodic potential. With the Lyapunov exponent, we find that there exists a critical region in the parameter λ-E plane. The critical region consists of critical states. In comparison with localized and extended states, the fluctuation of spatial extensions of the critical states is much larger. The numerical results show that the scaling exponent of inverse participation ratio (IPR) of critical states $x \simeq 0.5$. Furthermore, it is found that the critical indices of localized length $\nu = 1$ for the bounded ($|\alpha| < 1$) case and $\nu = 1/2$ for the unbounded ($|\alpha| \geqslant 1$) case. The above distinct critical indices can be used to distinguish the localized-extended from localized-critical transitions. At the end, we show that the systems with different E for both cases of $|\alpha| < 1$ and $|\alpha| \geqslant 1$ can be classified by the Lyapunov exponent $\gamma(E)$ and Avila's quantized acceleration $\omega(E)$.

DOI: 10.1103/PhysRevB.105.174206

I. INTRODUCTION

For a conventional orthogonal class system, it is believed that an arbitrarily weakly uncorrelated diagonal disorder in one and two dimensions [1] can result in the Anderson localization [2], that all the eigenstates are localized. However, in the presence of off-diagonal disorders, a one-dimensional system can have extended states [3,4]. In three dimensions, there exists mobility edge E_c which separates the localized states from extended states [5]. When the energies approach the mobility edge E_c, the localized length of localized states would diverge.

In one dimension, a famous example where the localized-extended transition can occur is the Aubry-André lattice model (AA model) [6], i.e.,

$$t[\psi(i+1)+\psi(i-1)]+2\lambda\cos(2\pi\beta i+\phi)\psi(i)=E\psi(i), \tag{1}$$

where t is hopping, $i \in Z$ is the lattice site index, 2λ describes the quasiperiodic potential strength, β is an irrational number, and ϕ is a phase. When the quasiperiodic potential is weak, i.e., $|\lambda/t| < 1$, all the eigenstates are extended states. When the potential strength is sufficiently large ($|\lambda/t| > 1$), all the eigenstates become localized states with a localized length $\xi = 1/\ln(\lambda/t)$. At the critical point ($|\lambda/t| = 1$), all the eigenstates are critical states. So there is no mobility edge in the AA model. The nonexistence of mobility edges originates from exact self-duality of this model at the critical point. In general, the breaking of the self-duality would result in the appearance of mobility edges in the one dimensional system [7–16].

A generalized Aubry-André model (GAA model) which can have mobility edges has been proposed by Ganeshan *et al.* [17–21]. The GAA model is

$$t[\psi(i+1)+\psi(i-1)]+\frac{2\lambda\cos(2\pi\beta i+\phi)}{1-\alpha\cos(2\pi\beta i+\phi)}\psi(i) = E\psi(i). \tag{2}$$

In comparison with the AA model, there is an extra parameter α which is a real number. Surprisingly, the mobility edges can be exactly obtained with a generalized self-dual transformation. Later, the mobility edges have been experimentally observed [22]. Very recently, a so-called mosaic model has been proposed [23] which also has mobility edges and localized-extended transitions. The Lyapunov exponent and mobility edges can be exactly obtained with Avila's global theory on the single frequency quasiperiodic potentials [24,25].

In the previous studies (for example, in Refs. [17,25]), the parameter α in the GAA model is limited to $|\alpha| < 1$ due to the concerns of the possible appearance of divergences in the quasiperiodic potential [see Eq. (2)]. A natural question arises: aside from the unboundedness of potential, how is it if $|\alpha| \geqslant 1$? One may wonder whether there exist mobility edges for $|\alpha| \geqslant 1$. What are the localized properties of eigenstates?

In this work, we try to answer the above questions by extending the previous investigations of the GAA model into a regime where parameter $|\alpha| \geqslant 1$. It is found that there are also mobility edges E_c. The Lyapunov exponent $\gamma(E)$ and mobility edges are also exactly obtained with the Avila's theory. In addition, we find that when $|\alpha| \geqslant 1$, in the parameter (λ, E) plane, a critical region which consists of critical states would appear. In comparison with the localized and extended states, the extensions of eigenstates in the critical region have

*Corresponding author: zhangyicai123456@163.com

 ©2022 American Physical Society

much larger fluctuations. Near the mobility edges, there exist localized-critical transitions where the localized length becomes infinite, e.g.,

$$\xi(E) \equiv 1/\gamma(E) \propto |E - E_c|^{-\nu} \to \infty, \quad \text{as } E \to E_c, \tag{3}$$

where the critical index [26] $\nu = 1/2$, which is different from that ($\nu = 1$) of the case of $|\alpha| < 1$. Finally, we find that the systems with different parameter E can be systematically classified by Lyapunov exponent and Avila's acceleration.

The work is organized as follows. First of all, we discuss the properties of eigenenergies of Hamiltonian operators for both $|\alpha| < 1$ and $|\alpha| \geqslant 1$ in Sec. II. In Sec. III, the Lyapunov exponents are obtained with Avila's theory. Next, with the Lyapunov exponent, we determine the mobility edges and critical region in Sec. IV. At the end, a summary is given in Sec. V.

II. BOUNDED AND UNBOUNDED ENERGY SPECTRUM OF GAA MODEL

Equation (2) can be viewed as an eigenequation of Hamiltonian operator H, i.e.,

$$H|\psi\rangle = (H_0 + V_p)|\psi\rangle = E|\psi\rangle, \tag{4}$$

where the free particle part H_0 and potential V_p in a second-quantized form are

$$H_0 = t\sum_i [C_{i+1}^\dagger C_i + C_i^\dagger C_{i+1}],$$
$$V_p = \sum_i \frac{2\lambda\cos(2\pi\beta i + \phi)}{1 - \alpha\cos(2\pi\beta i + \phi)} C_i^\dagger C_i, \tag{5}$$

where C_i ($C_i^\dagger$) is the annihilation (creation) operator for the state at site i.

A. $|\alpha| < 1$

When $|\alpha| < 1$, for an arbitrary integer i, due to $1 - \alpha\cos(2\pi\beta i + \phi) > 0$, the potential energy $\frac{2\lambda\cos(2\pi\beta i+\phi)}{1-\alpha\cos(2\pi\beta i+\phi)}$ is bounded. So, the Hamiltonian H is a bounded operator. For an arbitrary state $|\psi\rangle$, the average value of energy $\langle H\rangle$ is finite, i.e., there exists a real number $M > 0$, and the relation

$$|\langle H\rangle| = \frac{|\langle\psi|H|\psi\rangle|}{\langle\psi|\psi\rangle} < M \tag{6}$$

holds. Consequently, all the eigenvalues E_n of H ($H|\psi_n\rangle = E_n|\psi_n\rangle$) are finite, i.e.,

$$|E_n| < M, \tag{7}$$

also holds.

B. $|\alpha| \geqslant 1$

When $|\alpha| \geqslant 1$, due to the ergodicity of the map $\phi \longrightarrow 2\pi\beta i + \phi$ [27], $|1 - \alpha\cos(2\pi\beta i + \phi)|$ can be arbitrarily small if the lattice size is sufficiently large. Then the potential energy $\frac{2\lambda\cos(2\pi\beta i+\phi)}{1-\alpha\cos(2\pi\beta i+\phi)}$ can be arbitrarily large and the Hamiltonian H is an unbounded operator. So the average value of energy $\langle H\rangle$ is unbounded, i.e., for an arbitrary real number $M > 0$, there exists a state $|\psi\rangle$, and the relation

$$|\langle H\rangle| = \frac{|\langle\psi|H|\psi\rangle|}{\langle\psi|\psi\rangle} > M \tag{8}$$

holds. Consequently, the set of eigenvalues E_n of H is also unbounded. Namely, for an arbitrary real number $M > 0$, there exists an eigenenergy E_n, and the relation

$$|E_n| > M \tag{9}$$

holds.

TABLE I. The unboundedness of energy spectrum for $\alpha = 2$ and $\lambda = t$. We calculate the maxima of the absolute values of eigenenergies for lattice sizes $N = 100, 300, 500$ and $N = 700$, respectively. In our numerical calculations, we always take irrational number $\beta = \frac{\sqrt{5}-1}{2}$, phase $\phi = 0$, and hopping $t = 1$.

Lattice size	$N = 100$	$N = 300$	$N = 500$	$N = 700$
$\text{Max}\{\lvert E_n\rvert/t\}$	39.97	64.44	402.97	1186.65

The above results have been verified by our numerical calculations. To be specific, we take total lattice site number $N > 0$ and an $N \times N$ matrix associated with H can be established with open boundary conditions at two end sites. Then we diagonalize it to get the N eigenenergies and eigenstates. In our whole paper, we use the units of $t = 1$ and take irrational number $\beta = \frac{\sqrt{5}-1}{2}$ and phase $\phi = 0$. For $\alpha = 2$, we calculate the maxima of the absolute values of eigenenergies for lattice sizes $N = 100, 300, 500$ and $N = 700$, respectively. The results are reported in Table I. From Table I, we see that the maxima of eigenenergies of $\alpha = 2$ ($|\alpha| \geqslant 1$) grow rapidly with the increasing of lattice size N. It is expected when lattice size $N \to \infty$, the range of eigenenergies would be infinitely large.

In addition, when $|\alpha| \geqslant 1$ and the potential energy $\frac{2\lambda\cos(2\pi\beta i+\phi)}{1-\alpha\cos(2\pi\beta i+\phi)}$ is sufficiently large, the free particle part H_0 is negligible in Eq. (4). Now the eigenenergies are determined mainly by the potential. So it is expected that when $|\alpha| \geqslant 1$, the eigenstates with large eigenenergies are localized states. Another intensively investigated example of an unbounded operator in one dimension is the Maryland model where all the eigenstates are localized [28–30]. Furthermore, due to the ergodicity of the map $\phi \longrightarrow 2\pi\beta i + \phi$, for a given sufficiently large real number $\tilde{E}$, there exist some i, and the potential $\frac{2\lambda\cos(2\pi\beta i+\phi)}{1-\alpha\cos(2\pi\beta i+\phi)}$ can be very near the real number $\tilde{E}$. Consequently, there also exists an eigenenergy E_n which would be also very near the real number $\tilde{E}$. To be more precise, for an arbitrarily small real number $\delta > 0$, there exists a real number $M_\delta > 0$ (M_δ usually depends on δ), when $|\tilde{E}| > M_\delta$, and there exists an eigenenergy E_n, such that the relation

$$|E_n - \tilde{E}| < \delta \tag{10}$$

holds. Roughly speaking, there always exists an eigenenergy in a small neighborhood of a large real number. In this sense, we would say the set of eigenenergies is asymptotically dense in real number set R.

III. THE TRANSFER MATRIX AND THE LYAPUNOV EXPONENT

The localized properties of eigenstates can be characterized by the Lyapunov exponent. In this section, we present the transfer matrix method and its relation to the Lyapunov exponent.

First of all, we assume the system is a half-infinite lattice system with left-hand end sites $i = 0$ and $i = 1$. The Lyapunov exponent can be calculated with the transfer matrix method [31,32]. For example, using Eq. (2), starting from $\psi(0)$ and $\psi(1)$ of left-hand end sites, the wave function can be obtained with relation

$$\Psi(i) = T(i)T(i-1)\dots T(2)T(1)\Psi(0), \tag{11}$$

where matrix

$$T(n) \equiv \begin{bmatrix} \frac{E}{t} - \frac{2\lambda}{t}\frac{\cos(2\pi\beta n+\phi)}{1-\alpha\cos(2\pi\beta n+\phi)} & -1 \\ 1 & 0 \end{bmatrix} \tag{12}$$

and

$$\Psi(n) \equiv \begin{bmatrix} \psi(n+1) \\ \psi(n) \end{bmatrix}. \tag{13}$$

If one views Eq. (11) as an evolution equation of dynamical system, $\psi(0)$ and $\psi(1)$ would play the roles of the initial conditions.

For a given real number E, with the increasing of n, one can assume that the wave function would grow roughly according to an exponential law [33,34], i.e.,

$$\psi(n) \sim e^{\gamma(E)n}, \qquad \text{as } n \to \infty, \tag{14}$$

where $\gamma(E) \geqslant 0$ is Lyapunov exponent which measures the average growth rate of wave function. If the parameter E is not an eigenenergy of H, the Lyapunov exponent would be positive, $\gamma(E) > 0$ [35]. When the parameter E is an eigenenergy of H, the Lyapunov exponent can be zero or positive. For extended states (and critical states), the Lyapunov exponent $\gamma(E) \equiv 0$. While for localized states, the Lyapunov exponent $\gamma(E) > 0$.

Consequently, the Lyapunov exponent can be written as

$$\begin{aligned}\gamma(E) &= \lim_{L\to\infty} \frac{\ln(|\Psi(L)|/|\Psi(0)|)}{L} \\ &= \lim_{L\to\infty} \frac{\ln(|T(L)T(L-1)\dots T(2)T(1)\Psi(0)|/|\Psi(0)|)}{L},\end{aligned} \tag{15}$$

where L is a positive integer and

$$|\Psi(n)| = \sqrt{|\psi(n+1)|^2 + |\psi(n)|^2}. \tag{16}$$

The transfer matrix (12) can be further written as a product of two parts, i.e., $T(n) = A_n B_n$, where

$$\begin{aligned} A_n &= \frac{1}{1-\alpha\cos(2\pi\beta n+\phi)}, \\ B_n &= \begin{bmatrix} B_{11} & B_{12} \\ B_{21} & 0 \end{bmatrix}, \end{aligned} \tag{17}$$

with $B_{11} = \frac{E}{t}[1-\alpha\cos(2\pi\beta n+\phi)] - 2\lambda\cos(2\pi\beta n+\phi)/t$, and $B_{21} = -B_{12} = 1-\alpha\cos(2\pi\beta n+\phi)$. Now the Lyapunov exponent is

$$\gamma(E) = \gamma_A(E) + \gamma_B(E), \tag{18}$$

where

$$\gamma_A(E) = \lim_{L\to\infty} \frac{\ln(|A(L)A(L-1)\dots A(2)A(1)|)}{L} \tag{19}$$

and

$$\gamma_B(E) = \lim_{L\to\infty} \frac{\ln(|B(L)B(L-1)\dots B(2)B(1)\Psi(0)|/|\Psi(0)|)}{L}. \tag{20}$$

When $|\alpha| < 1$, the quasiperiodic potential is bounded and nonsingular. Avila's global theory would apply for such a case [24]. If parameter E is an eigenvalue of Hamiltonian H, the Lyapunov exponent can be obtained with Avila's theory [25]. When $|\alpha| \geqslant 1$, the Hamiltonian operator is unbounded due to the divergence of potential. Some conclusions of Avila's theory would not be valid for the unbounded case (see next section). Nevertheless, we would adopt a similar procedure to get the Lyapunov exponent and the Avila's acceleration (see next section). Their correctness would be verified by numerical calculations.

Following Refs. [25,36,37], first of all, we complexify the phase $\phi \to \phi + i\epsilon$ with $\epsilon > 0$, e.g., $B_{11} = \frac{E}{t}[1-\alpha\cos(2\pi\beta n+\phi+i\epsilon)] - 2\lambda\cos(2\pi\beta n+\phi+i\epsilon)/t$, and $B_{21} = -B_{12} = 1-\alpha\cos(2\pi\beta n+\phi+i\epsilon)$. In addition, due to the ergodicity of the map $\phi \longrightarrow 2\pi\beta n+\phi$, we can write $\gamma_A(E)$ as integral over phase ϕ [38], consequently

$$\begin{aligned}\gamma_A(E,\epsilon) &= \frac{1}{2\pi}\int_0^{2\pi} \ln\left(\frac{1}{|1-\alpha\cos(\phi+i\epsilon)|}\right)d\phi \\ &= \begin{cases} -\ln\left(\frac{1+\sqrt{1-\alpha^2}}{2}\right) & \text{for } |\alpha|<1 \;\&\; \epsilon < \ln\left(\frac{1+\sqrt{1-\alpha^2}}{|\alpha|}\right) \\ -\epsilon - \ln\left(\frac{|\alpha|}{2}\right) & \text{for } |\alpha| \geqslant 1. \end{cases}\end{aligned} \tag{21}$$

Next we take $\epsilon \to \infty$,

$$B_n = \frac{e^{-i(2\pi\beta n+\phi)+\epsilon}}{2}\begin{bmatrix} \frac{-(\alpha E+2\lambda)}{t} & \alpha \\ -\alpha & 0 \end{bmatrix} + O(1). \tag{22}$$

Then for large ϵ, i.e., $\epsilon \gg 1$, $\gamma_B(E,\epsilon)$ is determined by the largest eigenvalue (in absolute value) of B_n, i.e.,

$$\gamma_B(E,\epsilon) = \begin{cases} \epsilon + \ln\left(\frac{|P|+\sqrt{P^2-4\alpha^2}}{4}\right) & \text{for } P^2 > 4\alpha^2 \\ \epsilon + \ln\left(\frac{|\alpha|}{2}\right) & \text{for } P^2 < 4\alpha^2, \end{cases} \tag{23}$$

where

$$P = \frac{\alpha E + 2\lambda}{t}. \tag{24}$$

When ϵ is very small, using the facts that $\gamma(E,\epsilon) \geqslant 0$ and $\gamma(E,\epsilon)$ is a convex and piecewise linear function of ϵ [24,37], one can get

$$\begin{aligned}\gamma(E,\epsilon) &= \mathrm{Max}\{0, \gamma_A(E,\epsilon) + \gamma_B(E,\epsilon)\} \\ &= \begin{cases} \mathrm{Max}\left\{0, \epsilon + \ln\left(\frac{|P|+\sqrt{P^2-4\alpha^2}}{2|1+\sqrt{1-\alpha^2}|}\right)\right\}, & |\alpha| < 1 \ \&\ P^2 > 4\alpha^2 \\ 0, & |\alpha| < 1 \ \&\ P^2 < 4\alpha^2 \\ \ln\left(\frac{|P|+\sqrt{P^2-4\alpha^2}}{2|\alpha|}\right), & |\alpha| \geqslant 1 \ \&\ P^2 > 4\alpha^2 \\ 0, & |\alpha| \geqslant 1 \ \&\ P^2 < 4\alpha^2. \end{cases}\end{aligned} \tag{25}$$

Furthermore, when $\epsilon = 0$, the Lyapunov exponent $\gamma(E) \equiv \gamma(E, \epsilon = 0)$ is

$$\gamma(E) = \begin{cases} \mathrm{Max}\left\{0, \ln\left(\frac{|P|+\sqrt{P^2-4\alpha^2}}{2|1+\sqrt{1-\alpha^2}|}\right)\right\}, & |\alpha| < 1 \ \&\ P^2 > 4\alpha^2 \\ 0, & |\alpha| < 1 \ \&\ P^2 < 4\alpha^2 \\ \ln\left(\frac{|P|+\sqrt{P^2-4\alpha^2}}{2|\alpha|}\right), & |\alpha| \geqslant 1 \ \&\ P^2 > 4\alpha^2 \\ 0, & |\alpha| \geqslant 1 \ \&\ P^2 < 4\alpha^2. \end{cases} \tag{26}$$

The above generalized formula, Eq. (26), for both $|\alpha| < 1$ and $|\alpha| \geqslant 1$ has been verified by our numerical results (see Figs. 1 and 2).

In our numerical calculations, in order to get the correct Lyapunov exponents, on the one hand, the integer L should be sufficiently large. On the other hand, L should be also much smaller than the system size N, i.e., $1 \ll L \ll N$. To be specific, taking $\alpha = 1/2, 2$, $\lambda/t = 1, 3, 5$, system size $N = 1000$, we get the $N = 1000$ eigenenergies and eigenstates. Then, we calculate the Lyapunov exponents numerically for all the eigenenergies (see the several sets of discrete points in Figs. 1 and 2). In our numerical calculation, we take $L = 200$, phase $\phi = 0$, $\psi(0) = 0$, and $\psi(1) = 1$ in Eq. (15). The solid lines of Figs. 1 and 2 are given by Eq. (26) with the same parameters. It is shown that almost all discrete points fall onto the solid lines.

However, we also note that there are some discrete points of localized states which are not on the solid lines. This is because these localized wave functions are too near the left-hand boundary of the system.

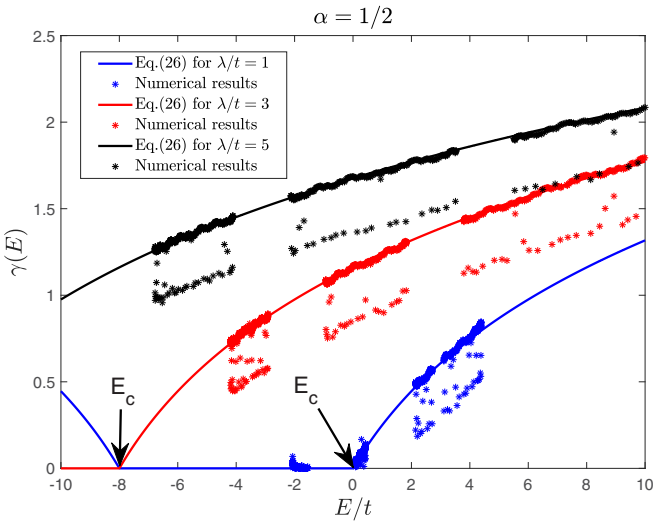

FIG. 1. Lyapunov exponents for the bounded case ($\alpha = 1/2$) and potential strength $\lambda/t = 1, 3, 5$. The discrete points are the numerical results for eigenenergies. The solid lines are given by Eq. (26). The mobility edges for $\lambda/t = 1$ are indicated by black arrows. Near mobility edges of the localized-extended transition (e.g., $E_c = 0$ and $-8t$ for $\lambda/t = 1$), the Lyapunov exponent $\gamma(E) \propto |E - E_c|$ approaches zero (as $E \to E_c$). The critical index of the localized length $\nu = 1$.

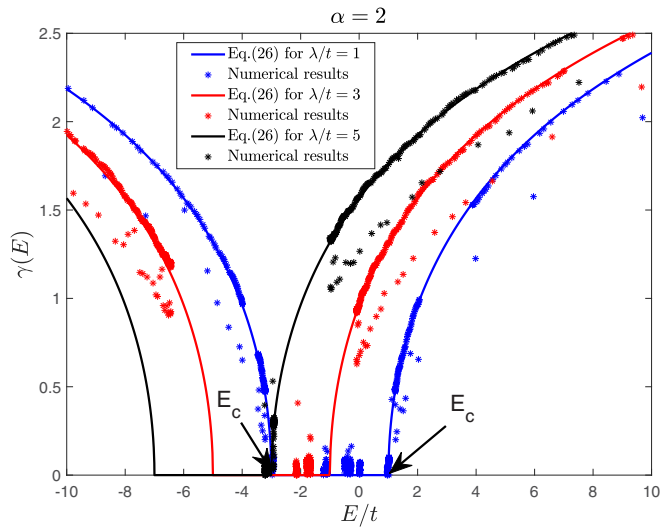

FIG. 2. Lyapunov exponents for the unbounded case ($\alpha = 2$) and potential strength $\lambda/t = 1, 3, 5$. The discrete points are the numerical results for eigenenergies. The solid lines are given by Eq. (26). The mobility edges for $\lambda/t = 1$ are indicated by black arrows. Near the localized-critical transition (e.g., $E_c = t$ and $-3t$ for $\lambda/t = 1$), the Lyapunov exponent $\gamma(E) \propto |E - E_c|^{1/2}$ (as $E \to E_c$), and the critical index of the localized length $\nu = 1/2$.

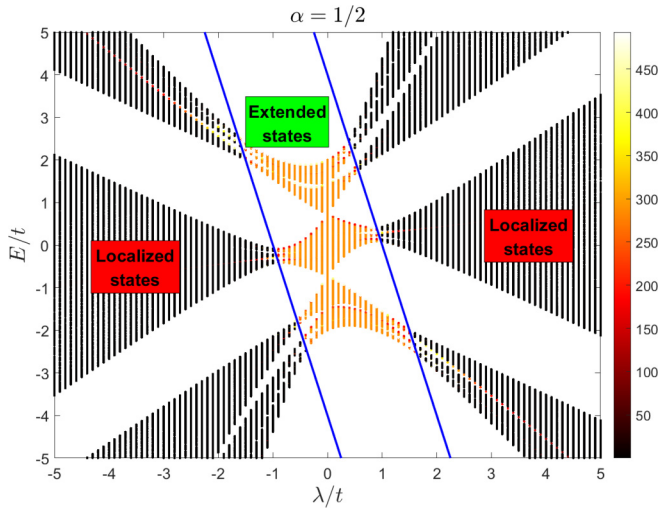

FIG. 3. Phase diagram in (λ, E) plane for the bounded case ($\alpha = 1/2$). When $\alpha = 1/2$, there exist localized-extended transitions. The blue solid lines are the phase boundaries (mobility edges E_c), which are given by Eq. (28). Standard deviations are represented with different colors.

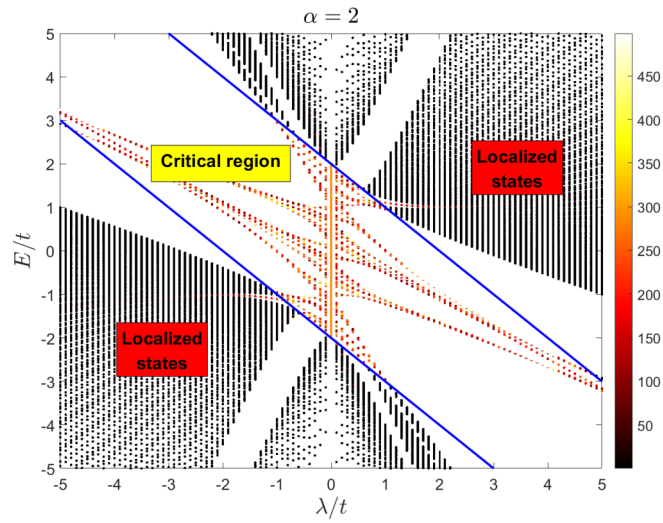

FIG. 4. Phase diagram in (λ, E) plane for the unbounded case ($\alpha = 2$). When $\alpha = 2$, there exist localized-critical transitions. The blue solid lines are the phase boundaries (mobility edges E_c), which are given by Eq. (33). Standard deviations are represented with different colors. Within the critical region, there are large fluctuations in standard deviations.

IV. THE MOBILITY EDGES AND CRITICAL REGION

In this section, based on the Lyapunov exponent formula Eq. (26), we determine the mobility edges and the critical region.

A. $|\alpha| < 1$

When $|\alpha| < 1$, there exist localized-extended transitions [17] (see Fig. 3). Based on Eq. (26), the mobility edges E_c which separate the localized from the extended states, are determined by [25]

$$\gamma(E_c) = \ln\left(\frac{|P| + \sqrt{P^2 - 4\alpha^2}}{2|1 + \sqrt{1-\alpha^2}|}\right) = 0. \tag{27}$$

Then

$$|P| = 2 \to \left|\frac{\alpha E_c + 2\lambda}{t}\right| = 2, \tag{28}$$

which is consistent with the result of Ganeshan *et al.* [17] for $|\alpha| < 1$. Furthermore, when $\alpha = 0$, the transition point is given by

$$|\lambda| = |t|, \tag{29}$$

which is reduced into the well-known Aubry-André's self-dual result [6].

By expanding the Lyapunov exponent near the mobility edges E_c, we get

$$\gamma(E) \propto |E - E_c| \to 0, \qquad \text{as } E \to E_c. \tag{30}$$

Then the localized length is

$$\xi(E) \equiv 1/\gamma(E) \propto |E - E_c|^{-1} \to \infty, \qquad \text{as } E \to E_c. \tag{31}$$

Its critical index is 1 for the bounded case of $|\alpha| < 1$ (see the finite slopes of solid lines near E_c in Fig. 1), which is also consistent with the numerical findings [39,40]. When E is an eigenenergy and $E = E_c$, the state of E is a critical state. Because the energy $E = E_c$ is an isolated point of real number set R, the critical states at $E = E_c$ are usually unstable under perturbations [24].

B. $|\alpha| \geqslant 1$

When $|\alpha| \geqslant 1$, there are localized-critical transitions (see Fig. 4). The mobility edges E_c which separate the localized from the critical states, by Eq. (26), are determined by

$$P^2 = 4\alpha^2. \tag{32}$$

Then

$$|P| = 2|\alpha| \to \left|\frac{\alpha E_c + 2\lambda}{t}\right| = 2|\alpha|. \tag{33}$$

The critical region (see Fig. 4) is given by

$$|P| < 2|\alpha| \to \left|\frac{\alpha E + 2\lambda}{t}\right| < 2|\alpha|. \tag{34}$$

Near the mobility edges E_c, we find that the Lyapunov exponent behaves as

$$\gamma(E) \propto |E - E_c|^{1/2} \to 0, \qquad \text{as } E \to E_c. \tag{35}$$

Then the localized length is

$$\xi(E) \equiv 1/\gamma(E) \propto |E - E_c|^{-1/2} \to \infty, \qquad \text{as } E \to E_c. \tag{36}$$

Its critical index is 1/2 (see the infinitely large slopes of solid lines near E_c in Fig. 2).

Several typical wave functions for localized, critical, and extended states are reported in Fig. 5. We can see that the wave function of the extended state extends over the whole lattices, while the localized state only occupies finite lattice sites. The

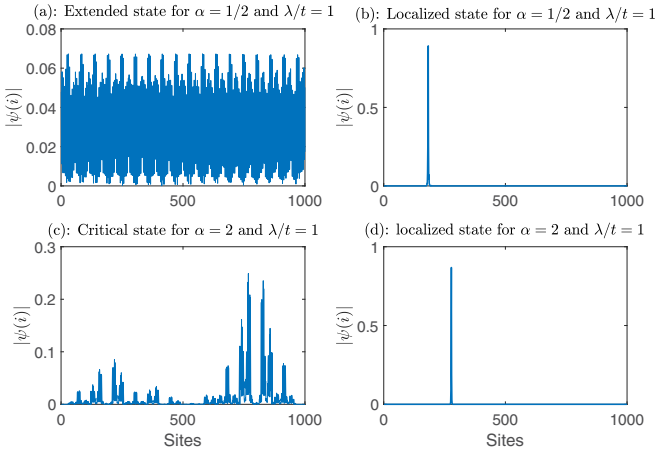

FIG. 5. Several typical wave functions for extended, localized, and critical states.

critical state consists of several disconnected patches which interpolate between the localized and extended states. In comparison with the extended states, there exist some unoccupied regions in the critical state wave function.

In order to further distinguish the localized states from the extended states (and critical states), we also numerically calculate the standard deviations of coordinates of eigenstates [11]

$$\sigma = \sqrt{\sum_i (i - \bar{i})^2 |\psi(i)|^2}, \tag{37}$$

where the average value of coordinate $\bar{i}$ is

$$\bar{i} = \sum_i i |\psi(i)|^2. \tag{38}$$

The standard deviation σ describes the spatial extension of wave function in the lattices. If one views E as a parameter,

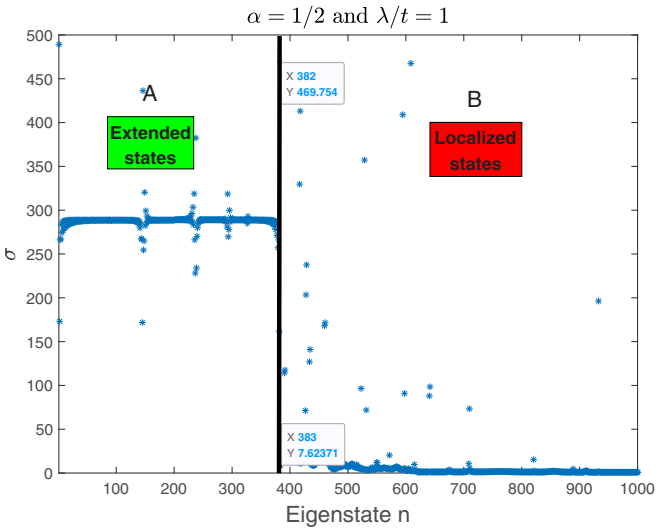

FIG. 6. Standard deviations of localized states and extended states for parameters $\alpha = 1/2$ and $\lambda/t = 1$. The eigenenergy E_n increases gradually as eigenstate index n runs from 1 to 1000.

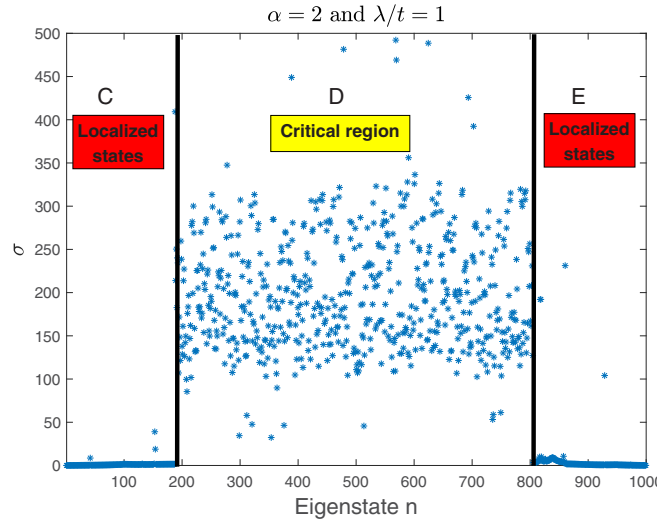

FIG. 7. Standard deviations of localized states and extended states for parameters $\alpha = 2$ and $\lambda/t = 1$. The eigenenergy E_n increases gradually as eigenstate index n runs from 1 to 1000.

a "phase diagram" in the (λ, E) plane can be obtained. The phase diagram is reported in Figs. 3 and 4. In Figs. 3 and 4, the standard deviations of coordinates are represented with different colors. From Figs. 3 and 4, we can see that when the states are localized, standard deviations of coordinates are very small. For extended states, the standard deviations are very large. The standard deviations of the critical states are in between of them (also see Figs. 6 and 7 and Table II).

For a given potential strength $\lambda/t = 1$, we report the standard deviations of eigenstates in Figs. 6 and 7. It is shown that in comparison with extended states and localized states, the critical states have much larger fluctuations of standard deviations. In order to see their differences, we calculate the fluctuation f_Ω for a given set of eigenstates Ω:

$$f_\Omega \equiv \sqrt{\sum_{k\in\Omega} (\sigma_k - \bar{\sigma}_\Omega)^2 / N_\Omega}, \tag{39}$$

where N_Ω is the total eigenstate number in set Ω and the average value of standard deviations

$$\bar{\sigma}_\Omega = \frac{1}{N_\Omega} \sum_{k\in\Omega} \sigma_k. \tag{40}$$

When $\alpha = 1/2$ and $\lambda/t = 1$, we take the set of extended states Ω_E where the state number runs from 1 to 382, i.e, region A of Fig. 6. When $\alpha = 2$ and $\lambda/t = 1$, we take the

TABLE II. The average values $\bar{\sigma}$ and their fluctuations for extended, localized, and critical states. The sets of extended states, localized states, and critical states correspond to regions A, C, and D of Figs. 6 and 7, respectively.

	Extended states	Localized states	Critical states
	$\alpha = 1/2$ & $\lambda/t = 1$	$\alpha = 2$ & $\lambda/t = 1$	$\alpha = 2$ & $\lambda/t = 1$
$\bar{\sigma}_\Omega$	287.94	1.19	199.77
f_Ω	20.78	3.16	68.86

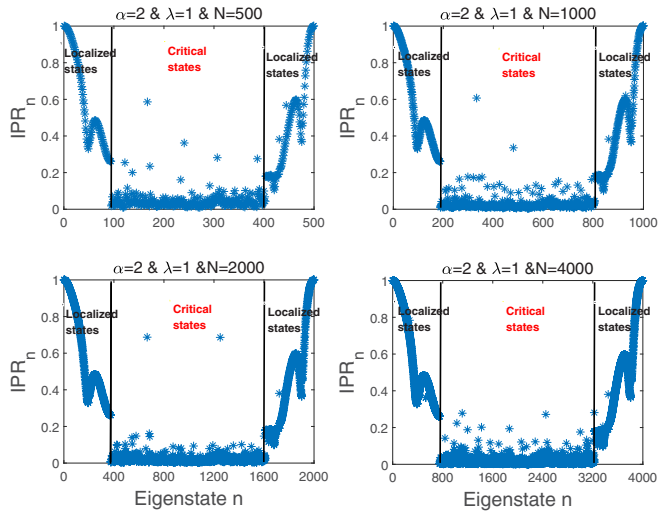

FIG. 8. The inverse participation ratio IPR_n of all the eigenstates for system size $N = 500$, 1000, 2000 and $N = 4000$.

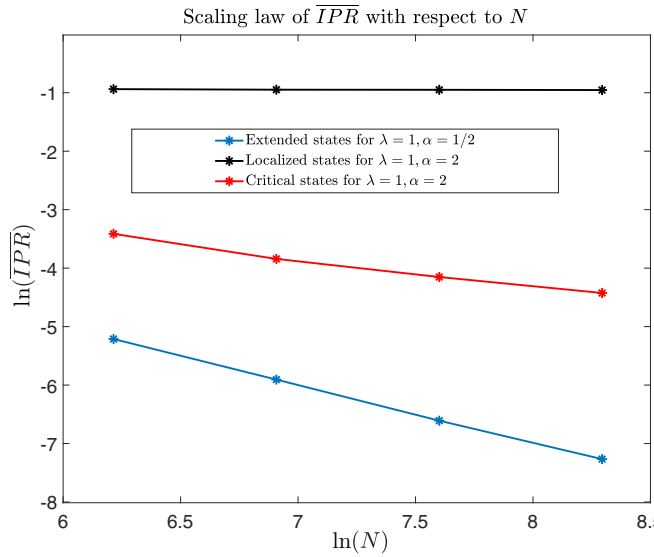

FIG. 9. The scaling law of $\overline{\mathrm{IPR}}$. We calculate the average participation ratio $\overline{\mathrm{IPR}}$ for the eigenstates in some typical energy intervals. The energy intervals for localized states, critical states, and extended states are $-3.5 < E/t < -3.2$, $-0.5 < E/t < -0.3$, and $-2.1 < E/t < -1.5$, respectively. The system sizes for the discrete points are $N = 500$, 1000, 2000 and $N = 4000$, respectively. It is found that for localized states, the scaling exponent $x \simeq 0$. While for extended states, the scaling exponent $x \simeq 1$. For critical states, the scaling exponent $x \simeq 0.5$.

set of localized states Ω_L where the state number runs from 1 to 187, i.e, region C of Fig. 7. For critical states, we take region D of Fig. 7 as a set of eigenstates Ω_{Cr}. The results are reported in Table II. It is shown that the fluctuation of critical states is much larger than that of the localized and extended states.

In order to investigate the properties of the wave functions of critical states, we also numerically calculate the inverse participation ratio IPR_n of all eigenstates for different system sizes $N = 500$, 1000, 2000 and $N = 4000$ [39,40], i.e.,

$$\mathrm{IPR}_n = \sum_i |\psi_n(i)|^4, \tag{41}$$

where $\psi_n(i)$ is the normalized wave function for the nth eigenstate. The results are reported in Fig. 8. We find that the IPRs of localized states are basically the same for different system sizes N, while the IPRs of critical states have much larger fluctuations.

On the whole, the IPR of critical states decreases with the increasing of system size N. The decreasing law may be captured by a power-law function

$$\overline{\mathrm{IPR}} \propto 1/N^x, \tag{42}$$

where $\overline{\mathrm{IPR}}$ is an average value of the IPR within a typical energy interval, and x is the scaling exponent. It is believed that, for localized states, the scaling exponent $x = 0$. While for extended states (like plane-wave states), the scaling exponent $x = 1$. For critical states, the exponent should be $0 < x < 1$ (see Fig. 9). For different system sizes N, due to the randomness of IPR of critical states (see Fig. 8), it is difficult to get a definite scaling exponent x. Here we find that for the critical states in the energy interval $-0.5 < E/t < -0.3$, the scaling exponent satisfies $0.39 < x < 0.62$, and its average value $\bar{x} \simeq 0.5$ (see Fig. 9).

C. Avila's acceleration

In addition, for the bounded quasiperiodic potentials, Avila also defined the acceleration $\omega(E)$ by [24]

$$\omega(E) = \lim_{\epsilon \to 0} \frac{\gamma(E, \epsilon) - \gamma(E, 0)}{\epsilon}. \tag{43}$$

Furthermore it is proved that acceleration $\omega(E) \geqslant 0$ and is quantized (an integer) for a bounded operator H. For critical states of $E = E_c$, $\gamma(E) = 0$ and $\omega(E) \neq 0$. Similarly, using Eqs. (25), when real number E is an eigenvalue of H, we extend it into the case of $|\alpha| \geqslant 1$ by

$$\omega(E) = \begin{cases} 1 \text{ for } |\alpha| < 1 \text{ \& energy of localized state} \\ 0 \text{ for } |\alpha| < 1 \text{ \& energy of extended state} \\ 1 \quad \text{for } |\alpha| < 1 \text{ \& energy of critical state} \\ 0 \qquad \text{for } |\alpha| \geqslant 1 \text{ \& if } E \text{ is eigenenergy.} \end{cases} \tag{44}$$

We note that that the second part of Eq. (21) is a linear function of ϵ, while the first part does not depend on ϵ. This is why accelerations $\omega(E)$ for $|\alpha| < 1$ and $|\alpha| \geqslant 1$ are different.

When $|\alpha| < 1$, by Avila's global theory [24], for an analytical (bounded) quasiperiodic potential, if the real number E is not an eigenvalue of Hamiltonian H, the Lyapunov exponent is always positive, i.e., $\gamma(E) > 0$ and the acceleration is always zero, i.e., $\omega(E) \equiv 0$. By further combining Eqs. (26) and (44), one can classify systems with different real parameter E (different phases) by Lyapunov exponent and the quantized

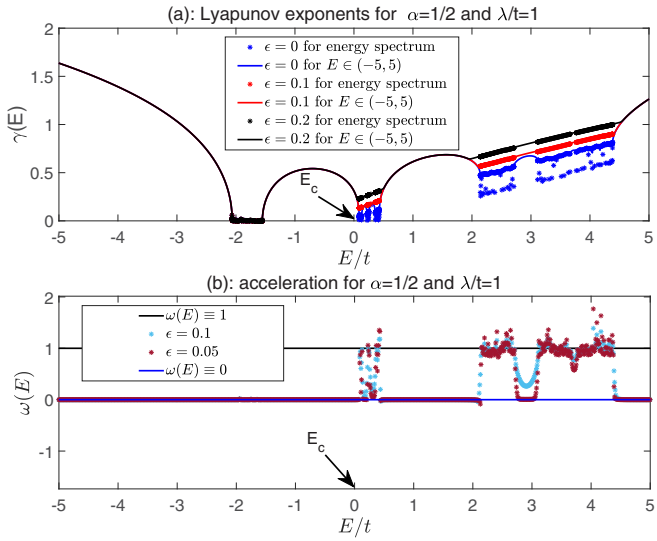

FIG. 10. Lyapunov exponents and Avila's accelerations for localized states and extended states. (a) Lyapunov exponents for $\alpha = 1/2$ and $\lambda/t = 1$. (b) Avila's accelerations for $\alpha = 1/2$. The mobility edges $E_c = 0$ are indicated by black arrows.

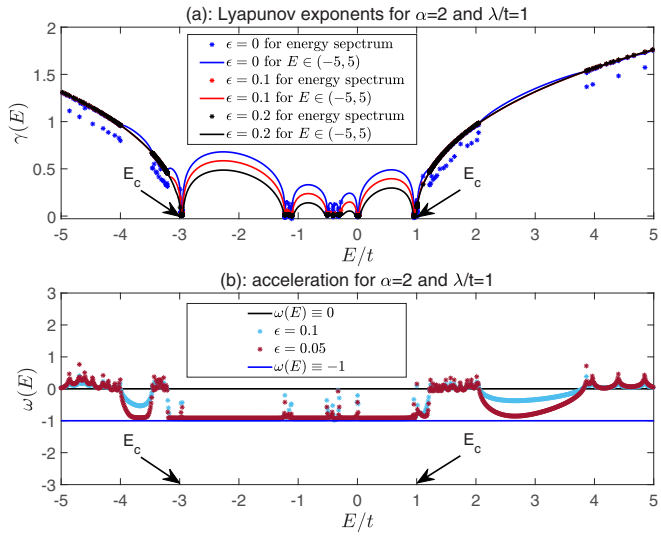

FIG. 11. Lyapunov exponents and Avila's accelerations for localized states and extended states. (a) Lyapunov exponents for $\alpha = 2$ and $\lambda/t = 1$. (b) Avila's accelerations for $\alpha = 2$. The mobility edges $E_c = -3t$ and t are indicated by black arrows.

acceleration, i.e.,

$$\begin{aligned}
&(a): \gamma(E) > 0 \ \ \& \ \omega(E) = 0 \text{ if } E \text{ is not an eigenvalue},\\
&(b): \gamma(E) > 0 \ \ \& \ \omega(E) = 1 \text{ for localized state},\\
&(c): \gamma(E) = 0 \ \ \& \ \omega(E) = 0 \text{ for extended state},\\
&(d): \gamma(E) = 0 \ \ \& \ \omega(E) = 1 \text{ for critical state}.
\end{aligned} \tag{45}$$

The above results are verified by our numerical calculations (see Fig. 10). To be specific, taking $\alpha = 1/2$, $\lambda/t = 1$, and $\epsilon = 0, 0.1, 0.2$, we calculate the Lyapunov exponents with Eq. (15) (taking the complexified phase $\phi \to \phi + i\epsilon = i\epsilon$) for interval $-5 \leqslant E \leqslant 5$ [see the three solid lines in panel (a) of Fig. 10]. In our calculation, we take $L = 200$, $\psi(0) = 0$, and $\psi(1) = 1$ in Eq. (15). At the same time, we calculate the Lyapunov exponents for all the eigenenergies with the same parameters [see the three sets of discrete points in panel (a) of Fig. 10]. We can find that if E is not an eigenenergy, its Lyapunov exponents are the same for all three different $\epsilon = 0, 0.1, 0.2$. When E is an eigenenergy of extended state [$\gamma(E) = 0$], the Lyapunov exponents are also the same for all three different $\epsilon = 0, 0.1, 0.2$. Whereas when E is an eigenenergy of localized state [$\gamma(E) > 0$], the Lyapunov exponents are different for three different $\epsilon = 0, 0.1, 0.2$. Their differences are linearly proportional to $\Delta\epsilon = 0.1$ in Fig. 10.

By taking $\epsilon = 0.1$ and $\epsilon = 0.05$, we also approximately calculate Avila's acceleration $\omega(E)$ by

$$\omega(E) \simeq \frac{\gamma(E, \epsilon) - \gamma(E, 0)}{\epsilon} \tag{46}$$

[see panel (b) of Fig. 10]. It shows that when E is an eigenenergy of localized state [$\gamma(E) > 0$], Avila's acceleration is 1. Otherwise, Avila's acceleration is 0.

Next we also carry a similar calculation for the case of $\alpha = 2$ ($|\alpha| \geqslant 1$) in panels (a) and (b) of Fig. 11. It is found that when E is not an eigenenergy, Avila's acceleration is -1. For other cases, Avila's acceleration is always 0. Consequently, for $|\alpha| \geqslant 1$, the systems with different real number E can be classified by

$$\begin{aligned}
&(a): \gamma(E) > 0 \ \ \& \ \omega(E) = -1 \text{ if } E \text{ is not eigenvalue},\\
&(b): \gamma(E) > 0 \ \ \& \ \omega(E) = 0 \text{ for localized state},\\
&(c): \gamma(E) = 0 \ \ \& \ \omega(E) = 0 \text{ for critical state},\\
&(d): \gamma(E) = 0 \ \ \& \ \omega(E) \neq 0 \text{ such } E \text{ does not exist}.
\end{aligned} \tag{47}$$

It is noted that Avila's acceleration is also quantized for the unbounded quasiperiodic potential in the GAA model. From Eqs. (45) and (47), we see Avila's acceleration can be used to distinguish the case (a) from case (b) of real number E.

V. SUMMARY

In conclusion, we extend the investigations of the GAA model into a regime of parameter $|\alpha| \geqslant 1$. It is found that there exist mobility edges which separate the localized states from critical states. Within the critical region, the spatial extensions of eigenstates have large fluctuations.

The Lyapunov exponents and mobility edges are exactly obtained with Avila's theory for both $|\alpha| < 1$ and $|\alpha| \geqslant 1$ cases. Furthermore, it is found that the critical index of localized length $\nu = 1$ for $|\alpha| < 1$, while for $|\alpha| \geqslant 1$, $\nu = 1/2$. The two different critical indices can be used to distinguish the localized-extended transitions from localized-critical transitions. The numerical results show that the scaling exponent of the IPR of critical states $x \simeq 0.5$. In addition, it is shown that the Lyapunov exponent and Avila's acceleration can be used to classify the systems with different E for both $|\alpha| < 1$ and $|\alpha| \geqslant 1$.

In some sense, we extend Avila's theory to unbounded quasiperiodic potentials in the GAA model. For example, we find that if E is not an eigenenergy, Avila's acceleration $\omega(E) = -1 < 0$, which is different from Avila's prediction

$[\omega(E) \geqslant 0]$ for bounded quasiperiodic potentials. In addition, when E is an eigenenergy of a localized state, it is found that $\omega(E) = 1$ for bounded quasiperiodic potentials, which is consistent with Avila's theory [$\omega(E)$ is a positive integer]. While for unbounded quasiperiodic potentials, we find that $\omega(E) = 0$ for localized states, which is also different from the bounded potential case. A much more exact theory for the unbounded quasiperiodic potential needs further investigations. We anticipate this work will spark further interests in the exact localization theory for the unbounded quasiperiodic potentials.

ACKNOWLEDGMENT

This work was supported by the NSFC under Grants No. 11874127 and No. 11774336.

[1] E. N. Economou, *Green's Functions in Quantum Physics*, 3rd ed. (Springer-Verlag, Berlin/Heidelberg, 2006).
[2] P. W. Anderson, Absence of diffusion in certain random lattices, Phys. Rev. **109**, 1492 (1958).
[3] G. Theodorou and M. H. Cohen, Extended states in a one-dimensional system with off-diagonal disorder, Phys. Rev. B **13**, 4597 (1976).
[4] P. D. Antoniou and E. N. Eeonomout, Absence of Anderson's transition in random lattices with off-diagonal disorders, Phys. Rev. B **16**, 3768 (1977).
[5] E. N. Economou and M. H. Cohen, Existence of mobility edges in Anderson's model for random lattices, Phys. Rev. B **5**, 2931 (1972).
[6] S. Aubry and G. André, Analyticity breaking and Anderson localization in incommensurate lattices, Ann. Isr. Phys. Soc. **3**, 133 (1980).
[7] S. Das Sarma, S. He, and X. C. Xie, Mobility Edge in a Model One-Dimensional Potential, Phys. Rev. Lett. **61**, 2144 (1988).
[8] T. Liu, G. Xianlong, S. Chen, and H. Guo, Localization and mobility edges in the off-diagonal quasiperiodic model with slowly varying potentials, Phys. Lett. A **381**, 3683 (2017).
[9] S. Sil, S. K. Maiti, and A. Chakrabarti, Metal-Insulator Transition in an Aperiodic Ladder Network: An Exact Result, Phys. Rev. Lett. **101**, 076803 (2008).
[10] Q. Tang and Y. He, Mobility edges in one-dimensional models with quasi-periodic disorder, J. Phys.: Condens. Matter **33**, 185505 (2021).
[11] D. J. Boers, B. Goedeke, D. Hinrichs, and M. Holthaus, Mobility edges in bichromatic optical lattices, Phys. Rev. A **75**, 063404 (2007).
[12] S. Das Sarma, S. He, and X. C. Xie, Localization, mobility edges, and metal-insulator transition in a class of one-dimensional slowly varying deterministic potentials, Phys. Rev. B **41**, 5544 (1990).
[13] X. Li, X. Li, and S. Das Sarma, Mobility edges in one-dimensional bichromatic incommensurate potentials, Phys. Rev. B **96**, 085119 (2017).
[14] F. M. Izrailev and A. A. Krokhin, Localization and the Mobility Edge in One-Dimensional Potentials with Correlated Disorder, Phys. Rev. Lett. **82**, 4062 (1999).
[15] H. P. Lüschen, S. Scherg, T. Kohlert, M. Schreiber, P. Bordia, X. Li, S. Das Sarma, and I. Bloch, Single-Particle Mobility Edge in a One-Dimensional Quasiperiodic Optical Lattice, Phys. Rev. Lett. **120**, 160404 (2018).
[16] F. Delyon, B. Simon, and B. Souillard, From Power-Localized to Extended States in a Class of One-Dimensional Disordered Systems, Phys. Rev. Lett. **52**, 2187 (1984).
[17] S. Ganeshan, J. H. Pixley, and S. Das Sarma, Nearest Neighbor Tight Binding Models with an Exact Mobility Edge in One Dimension, Phys. Rev. Lett. **114**, 146601 (2015).
[18] J. D. Bodyfelt, D. Leykam, C. Danieli, X. Yu, and S. Flach, Flatbands under Correlated Perturbations, Phys. Rev. Lett. **113**, 236403 (2014).
[19] A. Duthie, S. Roy, and D. E. Logan, Self-consistent theory of mobility edges in quasiperiodic chains, Phys. Rev. B **103**, L060201 (2021).
[20] J. Biddle and S. Das Sarma, Predicted Mobility Edges in One-Dimensional Incommensurate Optical Lattices: An Exactly Solvable Model of Anderson Localization, Phys. Rev. Lett. **104**, 070601 (2010).
[21] C. Danieli, J. D. Bodyfelt, and S. Flach, Flat-band engineering of mobility edges, Phys. Rev. B **91**, 235134 (2015).
[22] F. Alex An, K. Padavi, E. J. Meier, S. Hegde, S. Ganeshan, J. H. Pixley, S. Vishveshwara, and B. Gadway, Interactions and Mobility Edges: Observing the Generalized Aubry-André Model, Phys. Rev. Lett. **126**, 040603 (2021).
[23] Y. Wang, X. Xia, L. Zhang, H. Yao, S. Chen, J. You, Q. Zhou, and X.-J. Liu, One-Dimensional Quasiperiodic Mosaic Lattice with Exact Mobility Edges, Phys. Rev. Lett. **125**, 196604 (2020).
[24] A. Avila, Global theory of one-frequency Schrödinger operators, Acta Math. **215**, 1 (2015).
[25] Y. Wang, X. Xia, Y. Wang, Z. Zheng, and X.-J. Liu, Duality between two generalized Aubry-André models with exact mobility edges, Phys. Rev. B **103**, 174205 (2021).
[26] B. Huckestein and B. Kramer, One-Parameter Scaling in the Lowest Landau Band: Precise Determination of the Critical Behavior of the Localization Length, Phys. Rev. Lett. **64**, 1437 (1990).
[27] V. I. Arnold, *Mathematical Methods of Classical Mechanics*, 2nd ed. (Springer, New York, 1989).
[28] D. R. Grempel, S. Fishman, and R. E. Prange, Localization in an Incommensurate Potential: An Exactly Solvable Model, Phys. Rev. Lett. **49**, 833 (1982).
[29] B. Simon, Almost periodic Schrödinger operators IV. The Maryland model, Ann. Phys. **159**, 157 (1985).
[30] C. A. Marx and S. Jitomirskaya, Survey dynamics and spectral theory of quasi-periodic Schrödinger-type operators, Ergod. Theory Dyn. Syst. **37**, 2353 (2017).
[31] E. Sorets and T. Spencer, Positive Lyapunov exponents for Schrödinger operators with quasi-periodic potentials, Commun. Math. Phys. **142**, 543 (1991).
[32] P. S. Davids, Lyapunov exponent and transfer-matrix spectrum of the random binary alloy, Phys. Rev. B **52**, 4146 (1995).

[33] K. Ishii, Localization of eigenstates and transport phenomena in the one-dimensional disordered system, Prog. Theor. Phys. Suppl. **53**, 77 (1973).

[34] H. Furstenberg, Noncommuting random products, Trans. Am. Math. Soc. **108**, 377 (1963).

[35] R. A. Jonhnson, Exponential dichotomy, rotation number, and linear differential operators with bounded coefficients, J. Differ. Equations **61**, 54 (1986).

[36] Y. Wang and Z. Zheng, Coexistence of zero Lyapunov exponent and positive Lyapunov exponent for new quasi-periodic Schrödinger operator, arXiv:2009.06189.

[37] Y. Wang, X. Xia, J. You, Z. Zheng, and Q. Zhou, Exact mobility edges for 1D quasiperiodic models, arXiv:2110.00962.

[38] S. Longhi, Metal-insulator phase transition in a non-Hermitian Aubry-André-Harper model, Phys. Rev. B **100**, 125157 (2019).

[39] X. Li, J. H. Pixley, D.-L. Deng, S. Ganeshan, and S. Das Sarma, Quantum nonergodicity and fermion localization in a system with a single-particle mobility edge, Phys. Rev. B **93**, 184204 (2016).

[40] D.-L. Deng, S. Ganeshan, X. Li, R. Modak, S. Mukerjee, and J. H. Pixley, Many-body localization in incommensurate models with a mobility edge, Ann. Phys. **529**, 1600399 (2017).